

New Designs of Selective Multiplierless Cascaded-integrator-comb (CIC) Finite Impulse Response (FIR) Filter Functions

Atanas Tanev¹, Ivan Uzunov², Marin Hristov¹, Sotir Ouzounov³

¹Department of Microelectronics, Faculty of Electronic Engineering and Technologies
Techn. University - Sofia
8 Kl. Ohridski blvd., 1000
Sofia, Bulgaria
atanev@ecad.tu-sofia.bg; mhristov@ecad.tu-sofia.bg

²Smartcom Bulgaria AD, BIC IZOT, 133
Tzarigradsko Shosse blvd., 1784 Sofia
Bulgaria
ivan_uzunov@smartcom.bg

³Philips Research Europe, High Tech Campus
5656 AE Eindhoven, Netherlands
sotir.ouzounov@philips.com



ABSTRACT: *This paper has addressed the new designs of selective multiplierless Cascaded-Integrator-Comb (CIC) finite impulse response (FIR) filter functions with applications in modern communication systems. The cascading simple filters are used for designs. The resulting filters possess an improved frequency response behaviour. We have studied the influence of cosine prefilter and compensation filter to frequency response characteristics of proposed novel CIC FIR filter functions.*

Keywords: Ultra Low Voltage, Converter, Energy Harvesting, Sensors, Power Supply

Received: 3 September 2021, Revised 29 November 2021, Accepted 8 December 2021

DOI: 10.6025/jes/2022/12/1/16-24

Copyright: with Authors

1. Introduction

The optimization of the dynamic range is a significant problem in active filter design [1]. The problem in fact consists of two sub-problems, often solved simultaneously: maximizing the maximum permitted signal and minimizing the circuit noise. The maximum signal at the filter output is limited by the available voltage headroom and the acceptable level of distortions of the output signal. The methods for dynamic range optimization usually aim to equalize the output voltages of the amplifiers in the filter. However, the existing methods typically do not consider how the filter frequency response changes depending on of the amplifier nonlinearities.

The changes of the filter frequency response due to amplifiers' non-linearity are studied since a long time. The focus has been

on second-order bandpass filters due to their simplicity, considering basically gyrator equivalent of the LC tank [2,3] and a single operational amplifier biquad [4,5]. Their frequency response inclines at large input amplitudes (Fig. 1) due to nonlinearities in the active elements, which leads to three main effects: 1) The frequency response is no longer symmetric; 2) Its maximum moves usually to lower frequencies; 3) Appearance of the so called “jump phenomenon” at certain nonlinearity levels. The frequency response changes with a jump at a certain frequency and the suggestion is that it is due to appearance of area, in which the response has two values (dotted line in Figure 1).

Different techniques are applied for analysing the influence of the nonlinearities. In [2,3] analytical expressions are derived that link the level of non-linearity to the filter parameters in gyrator filters. In these studies, the operational transconductance amplifiers (OTA), used in the gyrator, are represented by equivalent large-signal value of the transconductances g_m where the g_m is impacted by the amplifier’s nonlinearity. More complicated methods have been proposed for achieving better accuracy and analysis the nonlinear effects in higher order filters. For example, the harmonic balance method is applied in [4,5], while in [6,7] Volterra series analysis is used. State-space analysis of the harmonic distortions in OTAC filters is considered in [8].

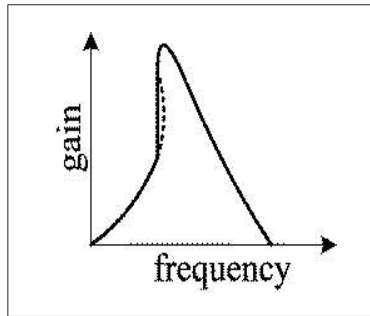


Figure 1. Inclining the frequency response and “jump phenomenon” in second-order band pass active filters due to amplifier nonlinearities

The review above shows that most of the existing methods for theoretical analysis of the nonlinear effects in the active filters are approximative and in most of the cases do not rely on powerful tools for simulation of electronic circuits like Cadence, PSpice, etc. Also, there are some questions that remain unclear. For example, the term “weak nonlinearities” is used without precise definition. Further, the relationship between the total harmonic distortion (THD) of the amplifiers and the variation of the filter frequency response it is not well clarified.

The goal of this paper is to study empirically these questions for one of the most popular bandpass filter – the gyrator parallel resonance circuit (gyrator tank). This is done by computer simulation of filter with different types of OTAs with different nonlinearity. The results demonstrate various effects in the frequency response and allow to estimate the limits of OTA’s THD in conjunction with the tolerable changes in the filter frequency response.

2. Gyrator Parallel Resonance Circuit and Modelling of OTAV-I Characteristic

The circuit of the bandpass filter, realized as parallel gyrator resonance circuit, is shown in Figure 2(a). The gyrator consists of g_{m1} and g_{m2} and forms the resonance circuit together with the capacitors C_1 and C_2 . OTA g_{m0} at the input converts the input voltage to an equivalent current for proper operation of the tank and R is the load resistance. The general form of the small-signal filter transfer function is

$$H(s) = \frac{V_o}{V_i} = \frac{hs\omega_0/Q}{s^2 + s\omega_0/Q + \omega_0^2}. \quad (1)$$

Its angular resonance frequency ω_0 , Q -factor and gain h are:

$$\omega_0 = \sqrt{\frac{g_{m1}g_{m2}}{C_1C_2}}; \quad Q = R\sqrt{\frac{g_{m1}g_{m2}C_1}{C_2}}; \quad h = g_{m0}R. \quad (2)$$

The corresponding frequency response is symmetrical around ω_0 when logarithmic scale is used for the frequency axes. Examples for two different Q -values are shown in Figure 2(b).

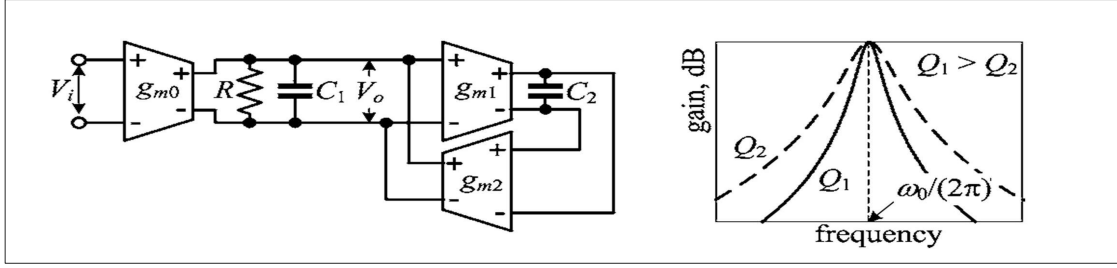


Figure 2. (a) Circuit of bandpass filter realized as parallel gyrator resonance circuit

(b) filter frequency response at two different pole Q factors

The investigation is focused on the impact of the nonlinearities in g_{m1} and g_{m2} on the filter frequency response. The harmonics produced in the input OTA g_{m0} typically are filtered by the gyrator tank. They may have visible effect only when the input signal is too large and the fundamental frequency of the signal is 2 or 3 times lower than $f_0 = \omega_0/(2\pi)$. For this reason this amplifier is considered as an ideal voltage controlled current source (VCCS). Its transconductance is equal to $1/R$ in all simulations in order to have unity gain at the filter central frequency f_0 .

The other two OTAs g_{m1} and g_{m2} are considered as nonlinear VCCS and their transfer characteristics $i_o(v_i)$ (i_o – OTA output current, v_i – OTA input voltage) are approximated by polynomials. Two different circuits are taken as models: the simple differential pair with dynamic load in Figure 3(a), and a differential amplifier with linearization (Figure 3(b)). The linearization of the second amplifier is achieved by source degeneration resistors – transistors M_3 - M_6 are used for this purpose. This amplifier also uses dynamic load. A negative resistance emulated by the pair M_9 - M_{10} is connected in parallel to the output for increasing the output impedance. The common mode feedback circuit (M_{cf1} - M_{cfA}) is shown also in Figure 3(b).

The studied circuit has been proposed in [9] and investigated in [10]. Its linearity is controllable by parameter a , equal to

$$a = \frac{(W/L)_{M1-2}}{(W/L)_{M3-6}}, \quad (3)$$

where $(W/L)_{M1-2}$ is the aspect ratio of transistors M_1 and M_2 and $(W/L)_{M3-6}$ of M_3 – M_6 . The value of a determines the achievable linearity and the best linearity is at an optimal a .

The $i_o(v_i)$ characteristics of the amplifiers is obtained by multiple time domain simulations with a sinusoidal voltage source at the input (terminals “ $+V_{in}$ ” and “ $-V_{in}$ ”), which amplitude is increased gradually. The output current flows through capacitor of 10nF, connected at the output (terminals “ $+V_o$ ” and “ $-V_o$ ”). The frequency is 10kHz and the capacitor impedance is about 1.6k Ω , which is much less than the amplifier output impedance – i.e. the capacitor realizes an approximate short circuit. The transfer characteristics are simulated with AMS 0.35 μm CMOS process used in the education. The sizes of all transistors are $W = 10 \mu\text{m}$, $L = 0.35 \mu\text{m}$ and only the widths of M_1 and M_2 are varied to achieve the desired parameter a . Tail currents I_{ss} are 35 μA for the circuit in Figure 3(a) and 100 μA in Figure 3(b). Their values are chosen in order to have approximately equal gm’s (about 150 μS) of both circuits. The simulated transfer characteristics are shown in Figure 4(a). Since they almost overlap for the amplifier in Figure 3(b), the dependence of THD from the input voltage, plotted in Figure 4(b), is used to demonstrate how the parameter a affect the linearity.

The next step is to receive an analytical approximation of the characteristics in Figure 4(a). Often is used tanh approximation, however the polynomial approximation is preferred here as more flexible, allowing to achieve of better accuracy. The OTAs are fully differential with symmetrical characteristics and the approximating polynomials are odd in the form

$$i_o = \alpha_1 v_i + \alpha_3 v_i^3 + \alpha_5 v_i^5 + \dots \quad (4)$$

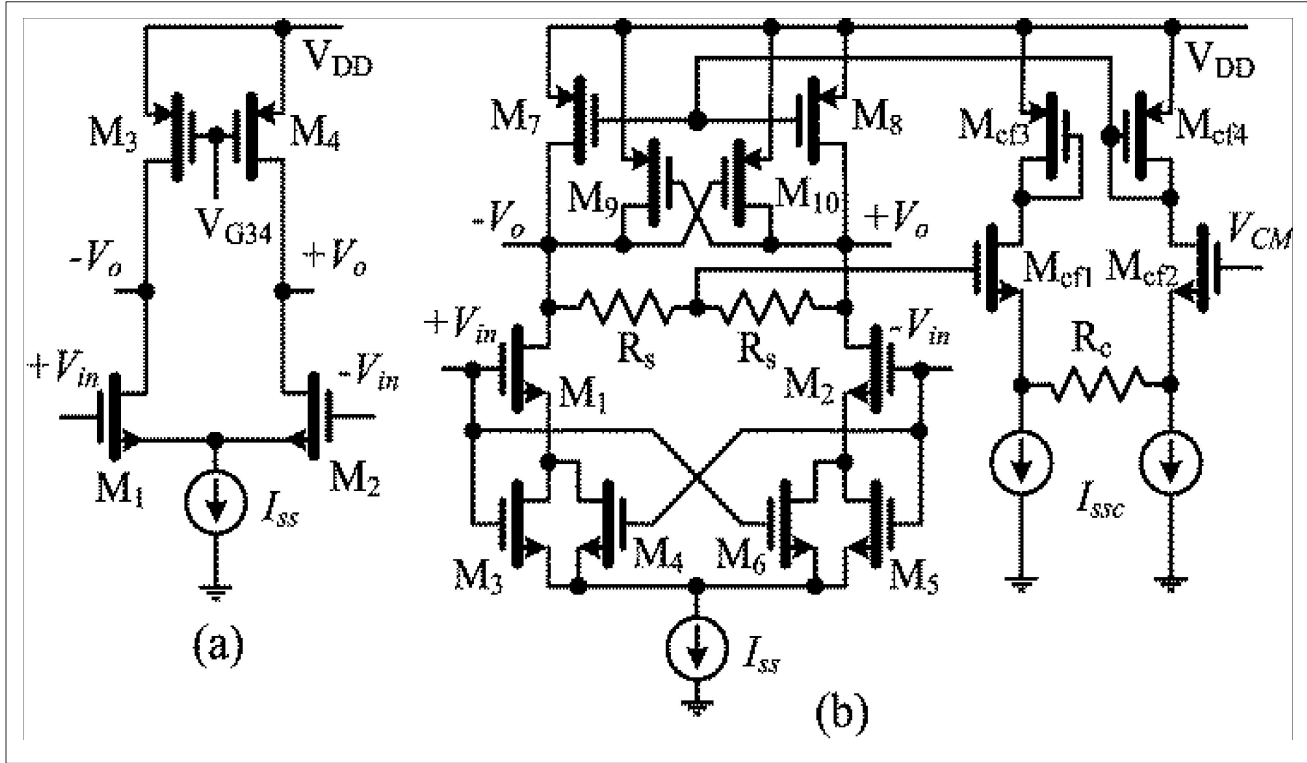


Figure 3. Circuits used for modelling of OTA nonlinearities: (a) simple differential pair; (b) differential amplifier with linearization

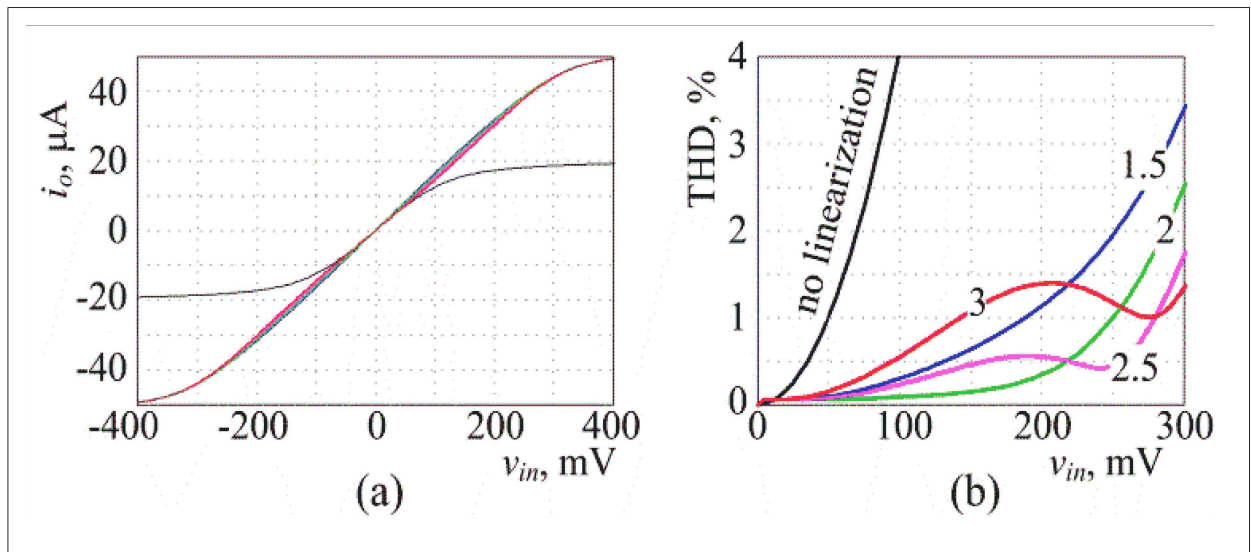


Figure 4. (a) Transfer characteristics $i_o(v_{in})$ of the amplifiers; (b) THD of the output current vs. input voltage v_{in} . Black curves are for the circuit in Figure 3(a). The others are for Figure 3(b). blue – $a = 1.5$, green – $a = 2$, magenta – $a = 2.5$, red – $a = 3$

The degree of polynomial is increased gradually until achieving relative approximation error of 1% for amplitudes of v_i up to 0.5V. The polynomial for the OTA in Figure 3(a) is: $i_o = 1.454 \times 10^{-4} \times v_i - 0.00242 \times v_i^3 + 0.0325 \times v_i^5 - 0.2694 \times v_i^7 + 1.296 \times v_i^9$, where v_i is in volts and i_o

is in amperes. The polynomials for the OTA with linearization are of 7th degree and their coefficients are given in Table 1.

Parameter a	α_1	α_3	α_5	α_7
1.5	0.0001648	-6.587×10^{-5}	-0.001995	0.004943
2	0.000158	8.857×10^{-5}	-0.003008	0.006985
2.5	0.0001503	0.0002396	-0.003932	0.008776
3	0.0001428	0.0003765	-0.004735	0.0103

Table 1. Coefficients of Approximating Polynomials for the Circuit in Figure 3(b)

3. Simulated Frequency Responses of the Nonlinear Gyrator Tank

Since the amplifiers, forming the gyrator, are nonlinear, time domain analysis should be used for obtaining their frequency characteristics. The small-signal resonance frequency of the gyrator tank is chosen as to be 800kHz in every simulation. A sinusoidal voltage source with amplitude V_{im} is applied at the input and the maximum of the output voltage V_{om} is determined by time-domain analysis. The gain in dB for the frequency of the source is calculated as $20 \log_{10}(V_{om}/V_{im})$. The frequency of the source is varied from 600kHz to 1MHz with step 1kHz and at each frequency is calculated the gain – in this way is obtained the large signal frequency response at the corresponding input amplitude.

The OTAs gm_1 and gm_2 are considered as nonlinear ideal VCCS, which dependencies $i_o(v_i)$ are given by the approximating polynomials received in the previous section. Both amplifiers are assumed with identical V-I characteristics. This approach allows to focus on the influence of the nonlinearity of the gm only. It also avoids the problems with adjusting the DC voltages at the points of connection of the amplifiers, which could misbalance their V-I characteristics.

The capacitors C_1 and C_2 are equal and their values are calculated from formula (2) in order to have 800kHz pole frequency, taking the transconductances gm_1 and gm_2 equal to the coefficient a_1 of the approximation polynomial. In order to evaluate the effect of nonlinearities at different Q-factors the simulations are done for $Q = 4, 10, 25$. Its value is adjusted by proper choice of the resistor R in Figure 2, changing correspondingly the value of gm_0 to keep $h = 1$.

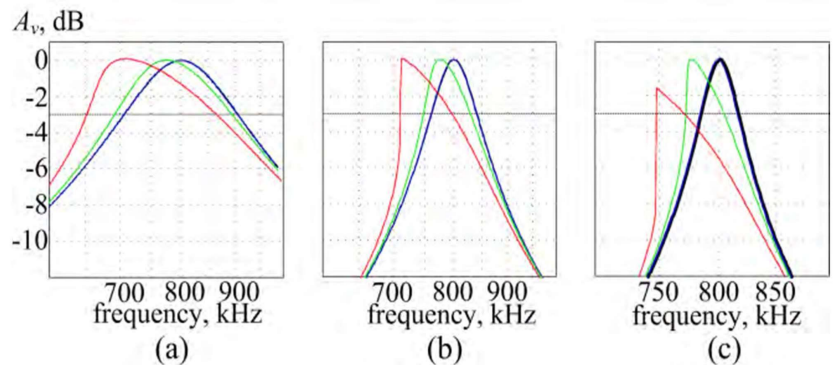


Figure 5. Frequency responses of the gyrator tank having amplifiers without linearization (Figure 3(a)). Colours: black – small signal (AC), blue – $V_{im} = 10\text{mV}$, green – $V_{im} = 50\text{mV}$, red – $V_{im} = 100\text{mV}$. (a) $Q = 4$; (b) $Q = 10$; (c) $Q = 25$

The linear frequency responses, received by AC analysis under the assumption of linear amplifiers, are the ideal case and they are used as reference for evaluation the changes of the other frequency responses due to nonlinearities. For this purpose, the corresponding AC frequency responses are added in every figure with black colour.

The results for gyrator resonance circuit having amplifiers without linearization are shown in Figure 5. When the input signal is small – 10mV, THD of the amplifiers is small (~0.3% according Fig. 4(b)) and corresponding curves practically overlap the AC

characteristics, i.e. the tank is still linear. Higher input amplitudes change the frequency response and its deviation is already visible when $V_{im} = 50\text{mV}$ (1% THD of the amplifiers).

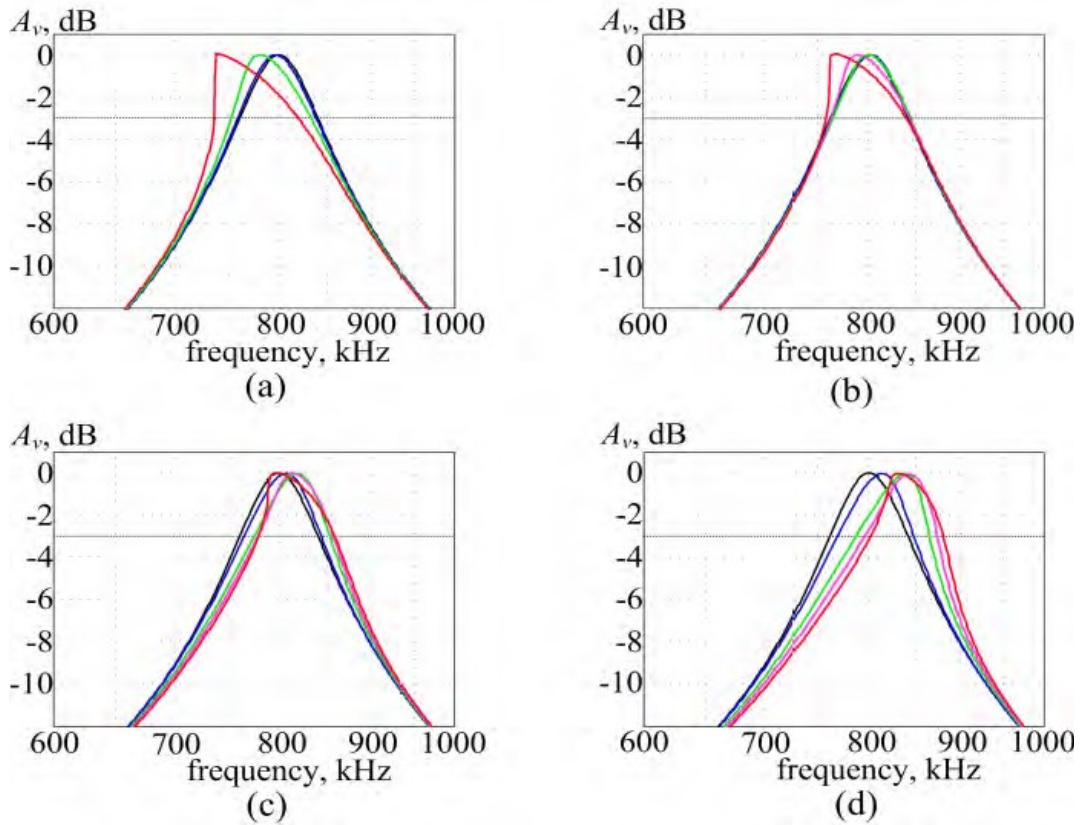


Figure 6. Frequency responses of the gyrator tank with $Q = 10$ and amplifiers with linearization. Colours: black – small signal (AC), blue – $V_{im} = 100\text{mV}$, green – $V_{im} = 200\text{mV}$, magenta – $V_{im} = 250\text{mV}$, red – $V_{im} = 300\text{mV}$. (a) Amplifiers with $a = 1.5$; (b) amplifiers with $a = 2$; (c) amplifiers with $a = 2.5$; (d) amplifiers with $a = 3$

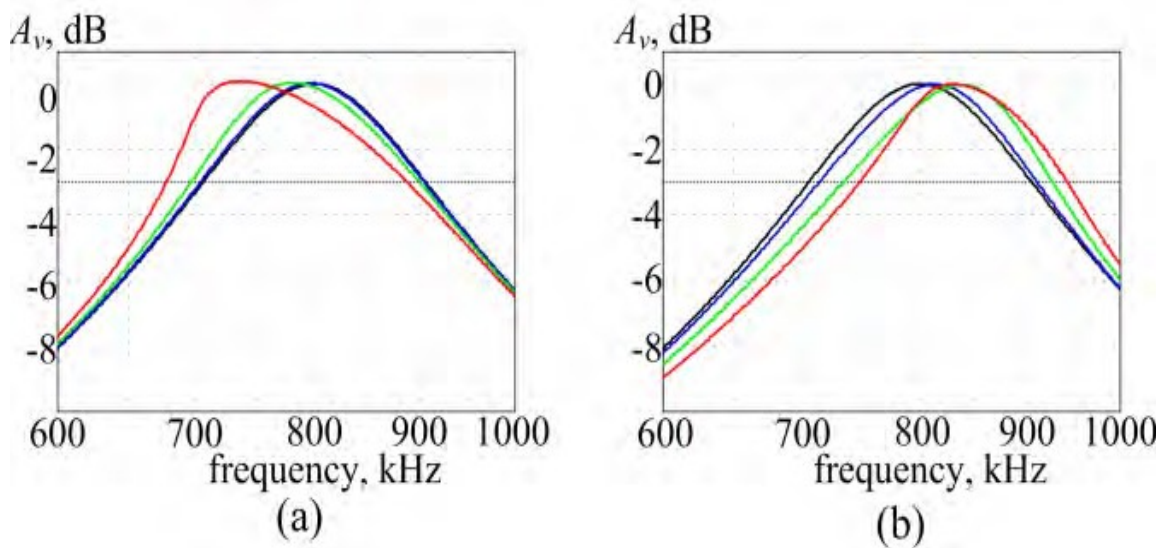


Figure 7. Frequency responses of the gyrator tank with $Q = 4$ and amplifiers with linearization. Colours: black – small signal (AC), blue – $V_{im} = 100\text{mV}$, green – $V_{im} = 200\text{mV}$, red – $V_{im} = 300\text{mV}$. (a) Amplifiers with $a = 1.5$; (b) amplifiers with $a = 3$

The use of linearized amplifier in Figure 3(b) as gyrator OTAs suggests more variants, since the OTA linearity can be controlled by the parameter a . Figure 6 shows the family of frequency responses when $Q = 10$ and $a = 1.5, 2, 2.5, 3$ (the same values of a as in Figure 4). Similar families when $Q = 4$ and $Q = 25$ are given in Figure 7 and Figure 8 correspondingly.

Several observations can be done from the simulations:

- 1) The OTA nonlinearities affect the filter frequency response basically around the resonance frequency. The change of the out of band suppression, especially when the attenuation is above 10 dB, is not large.
- 2) When the amplitude increases enough, the distorting of the frequency response is large and its maximum drops down significantly below the theoretical value of 0dB – e.g. the red curves in Figures 5(c), 8(a) and 8(b).
- 3) Most of the frequency responses move to lower frequencies when the signal increases. However, some of the curves when the parameter a is 2.5 or 3 move upward. This depends on the curvature of the function $i_o(v_{in})$, which is represented by its derivative di_o/dv_{in} , shown in Figure 9(a). When this derivative increases the frequency response moves upward; when it decreases the motion is opposite.

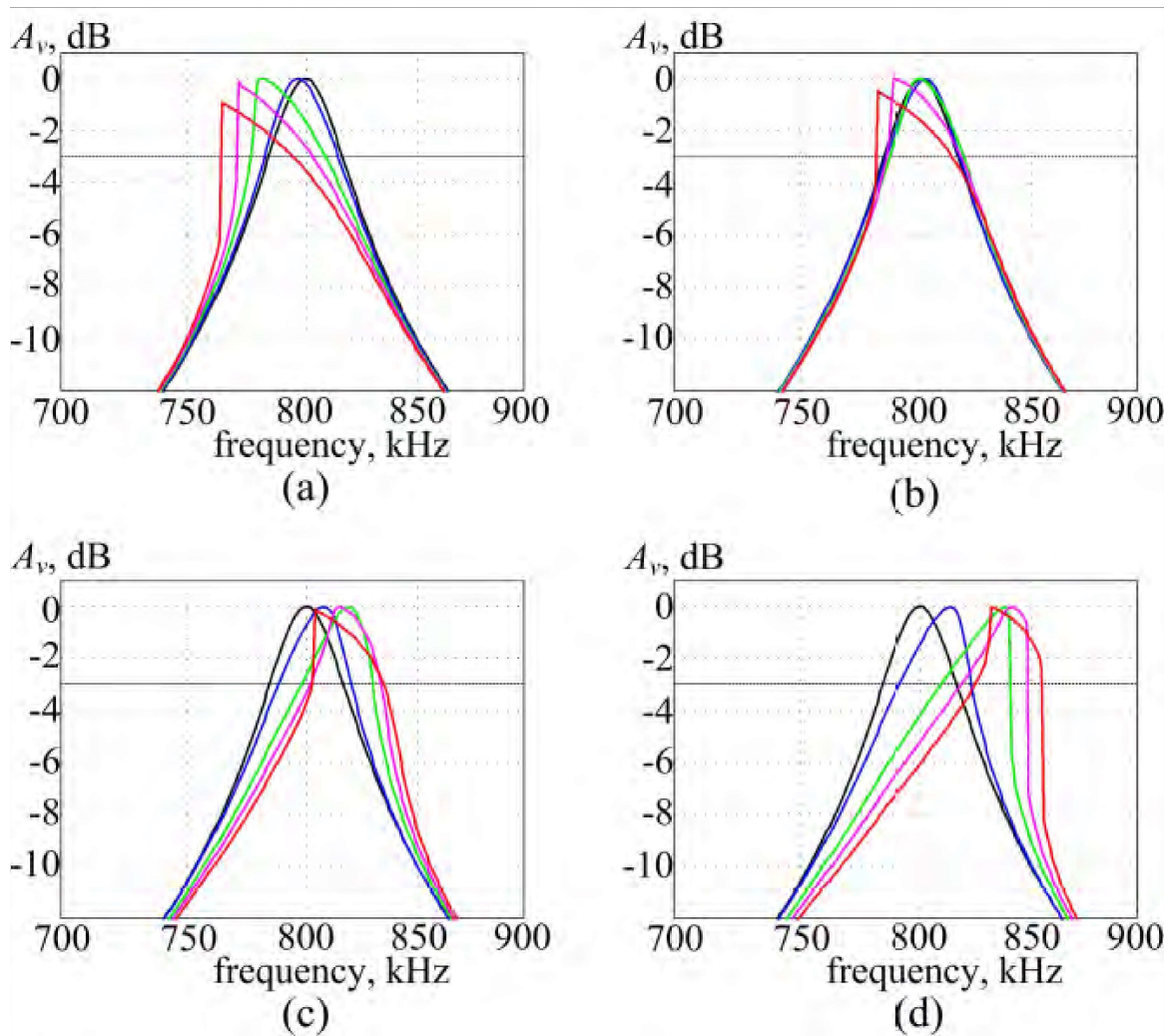


Figure 8. Frequency responses of the gyrator tank with $Q = 25$ and amplifiers with linearization. Colours: black – small signal (AC), blue – $V_{im} = 100\text{mV}$, green – $V_{im} = 200\text{mV}$, red – $V_{im} = 300\text{mV}$. (a) Amplifiers with $a = 1.5$; (b) amplifiers with $a = 2$; (c) amplifiers with $a = 2.5$; (d) amplifiers with $a = 3$

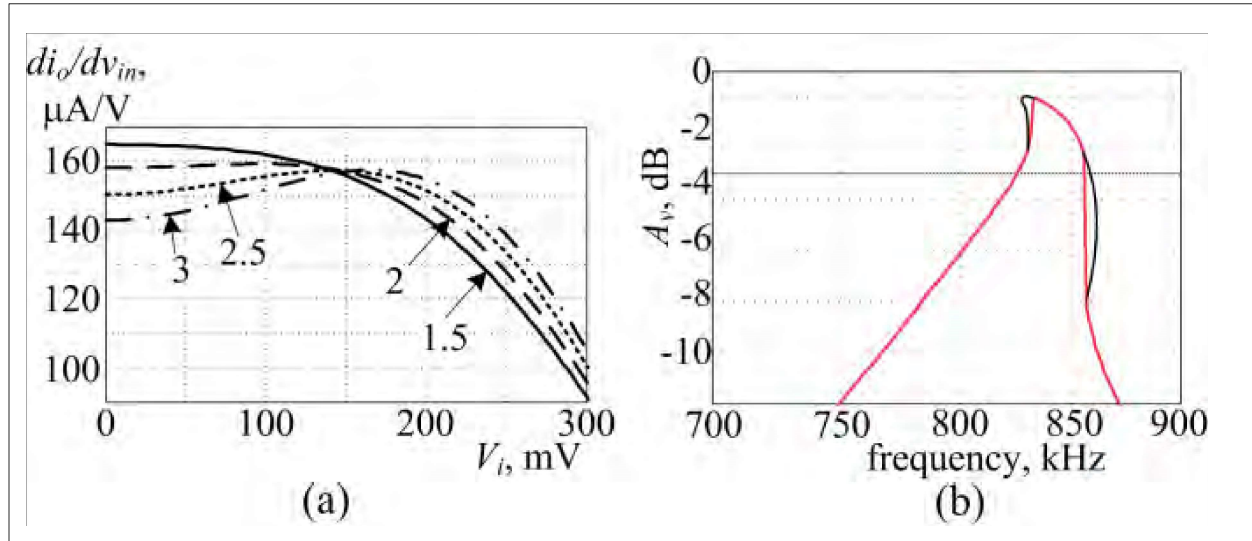


Figure 9. (a) Dependence of the derivative di_o/dv_{in} from the input voltage of the amplifier in Figure 3(b); (b) double inclining of the frequency response for $Q = 25$, $a = 3$, 300mV input signal

4) The change of the resonance frequency has very small dependence from the Q factor if there is no jump in the response. For example, when $a = 2.5$ and the input signal is 200mV, the maxima are at 816, 818, and 818kHz when $Q = 4, 10$ and 25 correspondingly. However the narrow bandwidth, when Q is high, makes the circuit more sensitive to the OTA nonlinearity.

5) An interesting case is the red curve in Figure 8(d), corresponding to $a = 3$ and 300mV input signal – it has two jumps. The large input signal covers areas, in which the differential g_m first increases and after that decreases (Figure 9(a)). This causes double inclining in the frequency response, shown with black lines in Figure 9(b).

6) The curves shows, that in the gyrator tank THD in the amplifiers above 0.5-0.6% cause undesired changes in its frequency response. However, this is not strict limit and it can vary depending on the Q , area of application and type of OTA nonlinearity.

4. Conclusions

A gyrator bandpass filters based of fully differential OTAs is investigated by computer simulation concerning the influence of OTA nonlinearity. The collected frequency responses allow to estimate a limit for THD of the amplifiers to 0.5% approximately when $Q < 10-15$. Then the resonance frequency changes by no more than 2-3% and the change of the frequency response is acceptable. It is observed also double inclining of the frequency response in some case – another interesting effects due to nonlinearity of amplifiers.

Acknowledgement

The research in this paper was carried out within the framework of Contract No. DUNK 01/03-12. 2009.

References

- [1] Deliyannis, T., Sun, Y., Fidler, J. K. (1999). Continuous-Time Active Filter Design, CRC Press, 1999.
- [2] Dinias, G., Deliyannis, T. (1975). Jump phenomenon in a gyrator circuit, *Electr. Letters*, 11 (23) 560-561, November 13.
- [3] Hiser, D. L., Geiger, R. L. (1990). Impact of OTA Nonlinearities on the Performance of Continuous Time OTA-C Filters Bandpass Filters, Proceedings of 1990 *Intern. Symp. Circuits and Systems (ISCAS)*, New Orleans, LA, US, May 1-3.
- [4] Bowron, P., Motlagh, M. R. J., Muhieddin, A. A. (1991). Harmonic characterization of feedback systems incorporating

saturation nonlinearities, *Electronic letters*, 27 (20) 1865-1867, September.

[5] Zeng, X., Bowron, P., Muhieddin, A. A. (1994). Nonlinear distortion prediction of active filters, *Electronic letters*, 30 (7) 553-554, March.

[6] Szczepanski, S., Schaumann, R. (1993). Nonlinearity-Induced Distortion of the Transfer Function Shape in High-Order OTA-C Filters, *Analog Integr. Circ. Signal Processing*, 3, 143-151.

[7] Cherry, J. A., Snelgrove, W. M. (1998). On the Characterization and Reduction of Distortion in Bandpass Filters, *IEEE Trans. Circuits and Systems – I: Fundamental Theory and Applications*, 45 (5) 523-537, May.

[8] Zhang, Z., Celik, A., Sotiriadis, P. (2006). State-Space Distortion Modeling A Weakly Nonlinear, Fully Balanced Gm-C Filters – A Modular Approach Resulting in Closed-Form Solutions, *IEEE Trans. Circuits and Systems – I: Regular Papers*, 53 (1) 48-59, January.

[9] Sun, Y., Jeong, C. J., Lee, I. Y., Lee, J. S., Lee, S. G. (2010). A 50-300 MHz Low Power and High Linear Active RF Tracking Filter for Digital TV Tuner ICs, *Proc. 2010 IEEE Custom Integrated Circuits Conf. (CICC 2010)*, San Jose, USA, 19-22 September 2010.

[10] Tanev, I., Uzunov, S., Ouzounov, M. Hristov. (2015). Computer Investigation of CMOS Operational Transconductance Amplifier (OTA) with Improved Linearity Implemented on AMS 0.35 μm Process, *Proceedings of XXIV Intern. Scient. Conf. Electronics – ET2015*, September, 15-17, Sozopol, Bulgaria.